Framework and grafted nickel ethylenediamine complexes in 2D hexagonal mesostructured templated silica

Wen-Juan Zhou,[a,b] Belén Albela,[a] Meigui Ou[c], Pascal Perriat[c], Ming-Yuan He[b] and Laurent Bonneviot[a*]

Electronic Supplementary Information

Coordination of nickel ethylenediamine complexes in the framework of mesostructured templated silica using a basic route

Wen-Juan Zhou [a,b], Belén Albela [a], Meigui Ou [c], Pascal Perriat [c], Ming-Yuan He [b] and Laurent Bonneviot [a*]

Table S1. UV-visible fingerprints of the complex before and after surfactant extraction according to methods *TA*, *T* and *TO*.

n

Sample	ν_2 ±50 cm^{-1}	ν_3 ±50 cm^{-1}
OP-Ni-3	17000	27400
OP-Ni-3TA	16900	27400
OP-Ni-3T	15700	26000
OP-Ni-3TO	14300	24450

ν_2 and ν_3 are the second and third d-d electronic transitions $^3T_{1g}(F) \rightarrow {}^3A_{1g}(F)$ and $^3T_{2g}(F) \rightarrow {}^3A_{1g}(F)$ respectively, assuming an octaedral symmetry for Ni(II), (*Scheme S1*).

Table S2. Nickel and silica content and molar ratios deduced from elemental analyses and weight loss from TGA.

Material	Ni [a] wt % ± 0.1	$SiO_{2\ inorg}$ [b] wt % ± 0.5	$Surf/Si_{inorg}$ [b,c] ± 0.01	TMS/Si_{inorg} [b] ± 0.01	L/Si_{inorg} [b] ± 0.01
OP-Ni-1	1.7	47.6	0.13	-	0.03
OP-Ni-2	1.6	48.3	0.11	-	0.07
OP-Ni-3	1.5	46.8	0.12	-	0.10
OP-Ni-1TA	2.2	64.2		0.25	0.03
OP-Ni-2TA	1.8	61.6		0.22	0.07
OP-Ni-3TA	1.9	56.7		0.24	0.09
OP	--	47.9	0.18	--	--
OP-TA	--	67.4		0.29	--
LUS-PSE	--	77.1		0.17	--
LUS-MSP-Ni-2	2.5	62.3		0.15	0.09
LUS-MSP-Ni-3	2.4	56.8		0.12	0.12

a: measured by ICP-MS; **b**: pure inorganic SiO_2 content obtained from the residual weight in TGA at 1000°C upon subtraction of both NiO and the SiO_2 formed from the grafted organosilanes, "**L**" means ligand (AAPTMS); **c**: surfactant (Surf) content is determined from nitrogen elemental analysis.

Table S3. Surface area and pore volume considering different residual mass.

Material	S_{BET} [a] ($m^2.g^{-1}$)±50	S_{BET} [b] ($m^2.g^{-1}$) ±50	S_{BET} [c] ($m^2.g^{-1}$) ±50
OP-TA	730	800	940
OP-Ni-1TA	600	750	930
OP-Ni-2TA	530	670	920
OP-Ni-3TA	470	610	840
LUS-MSP-Ni-2	600	788	982
LUS-MSP-Ni-3	550	681	965

Material	V_p [a] ($cm^3.g^{-1}$) ±50	V_p [b] ($cm^3.g^{-1}$) ±50	V_p [c] ($cm^3.g^{-1}$) ±50
OP-TA	0.70	0.77	0.90
OP-Ni-1TA	0.58	0.73	0.90
OP-Ni-2TA	0.52	0.66	0.90
OP-Ni-3TA	0.52	0.67	0.93
LUS-MSP-Ni-2	0.46	0.60	0.75
LUS-MSP-Ni-3	0.35	0.43	0.61

a: the reference mass includes all the organic and inorganic matter of the materials except water, measured after treatment of the sample at 80 °C under vacuum overnight (pre-treatment conditions of the N_2 sorption isotherm); **b**: includes all inorganic matter, *i.e.*, NiO and SiO_2 from both Ludox (inorganic) and organosilane (organic), obtained from the residual mass measured in TGA at 1000°C, *i.e.* residual SiO_2 and NiO; **c**: includes only inorganic silica.

Table S4. Parameters obtained from UV-visible for $Ni(Pren)_x$ complexes in aqueous solution.

Sample	ν_3 ±50 cm^{-1}	ν_2 ±50 cm^{-1}	**Δ** ±50 cm^{-1}	**β** ± 0.015
Solution, X = 1	26800	16100	9920	0.84
Solution X = 2	27800	17200	10790	0.81
Solution X = 3	27930	17360	10930	0.80
Solution X = 4	28100	17500	11040	0.80
Solution X = 6	28200	17500	11000	0.81
Solution X = 9	28300	17600	11090	0.81
Solution X = 18	28300	17600	11090	0.81

X= Pren/Ni molar ratio in the solution; **Δ**: calculated crystal field considering Oh symmetry; **β**: nephelauxetic parameter, $\beta = B/ B_0$; B, B_0: Racah parameters (Formula S1); B_0= 1041 cm^{-1} (Ni(II) free ion).

Formula S1:

Assuming an octahedral symmetry, β parameters can be determined from the following formulas: [1]

$\nu_3/\nu_2 = [15B+3*\Delta+(225*B^2-18*B*\Delta+\Delta^2)^{1/2}]/[15B+3\Delta-(225B^2-18*B*\Delta+\Delta^2)]$

$\nu_3/B = 1/2*[15+3*\Delta/\beta+(225-18*\Delta/\beta+(\Delta/\beta)^2)^{1/2}]$

$\nu_1 = \Delta$

Figure S1. UV-visible spectra of the Ni-AAPTMS complex (X=3) in aqueous solution at room temperature (**a**), 60 °C (**b**), 80 °C (**c**), 100 °C (**d**) and 130 °C (**e**)**.**

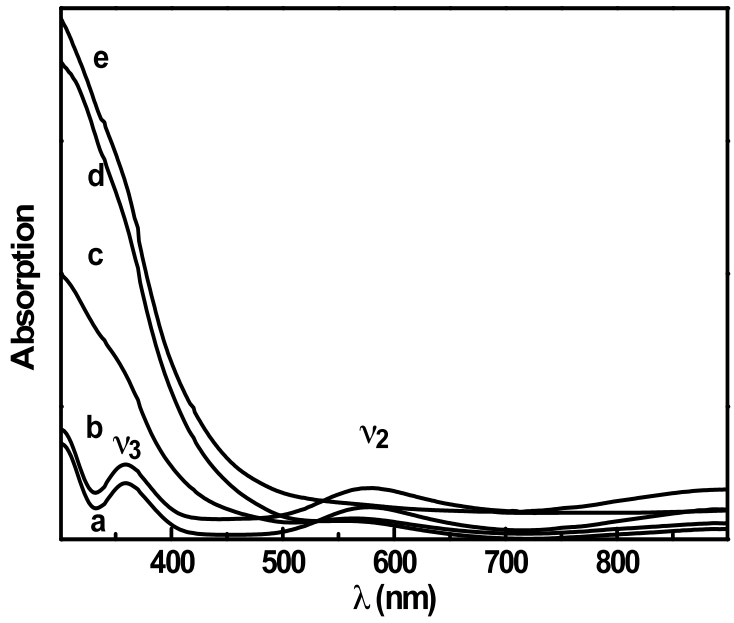

Figure S2. X-ray diffraction pattern of **OP**.

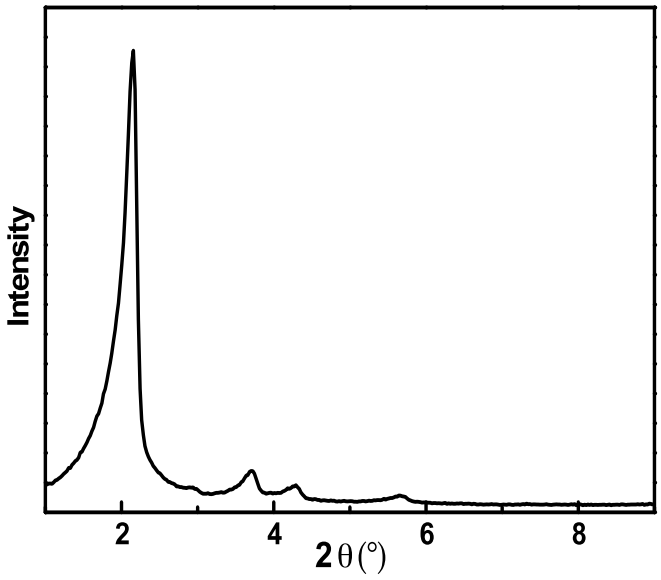

Figure S3. TGA diagram of **OP-Ni-3TA**, **OP-Ni-3T** and **OP-Ni-3TO**.

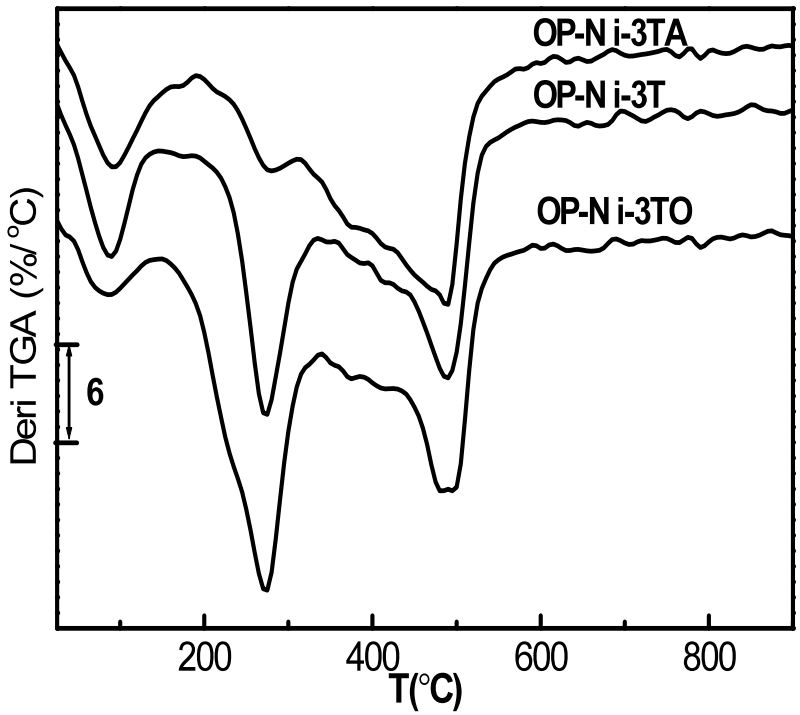

Figure S4. XRD patterns of **LUS-PSE** and **LUS-MSP-Ni-3**.

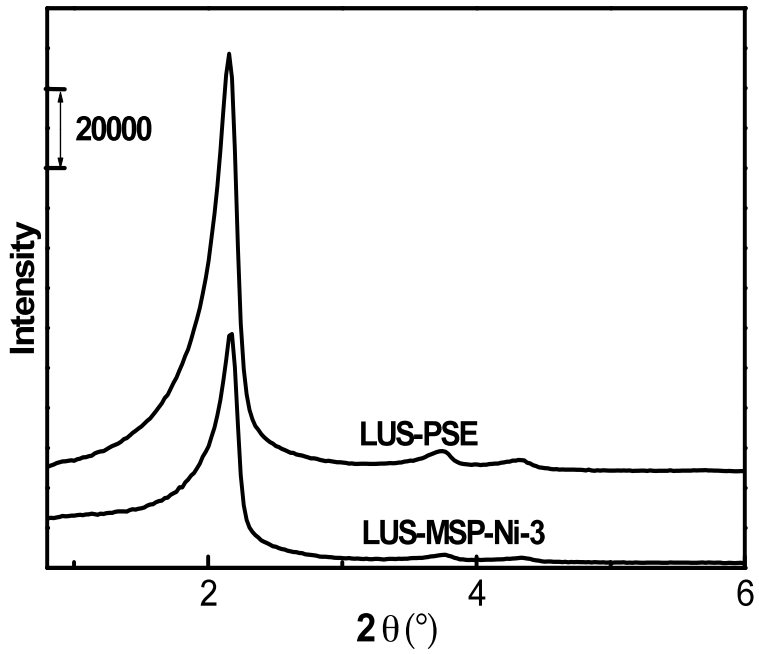

Figure S5. FT-IR spectra of **OP-Ni-3** and **OP-Ni-3TA** .

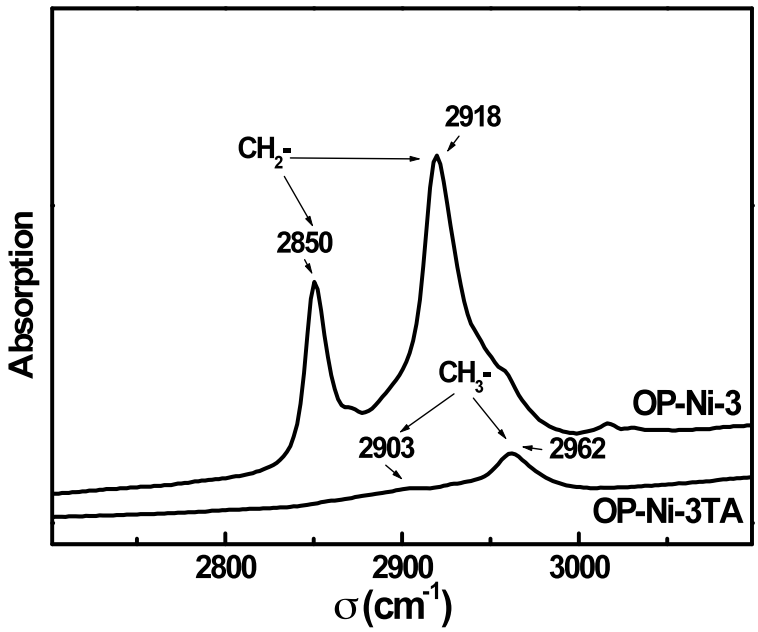

Figure S6. Absorption UV-visible bands of **LUS-MSP-Ni-2**, **LUS-MSP-Ni-2H** and **LUS-MSP-Ni-2HCu**.

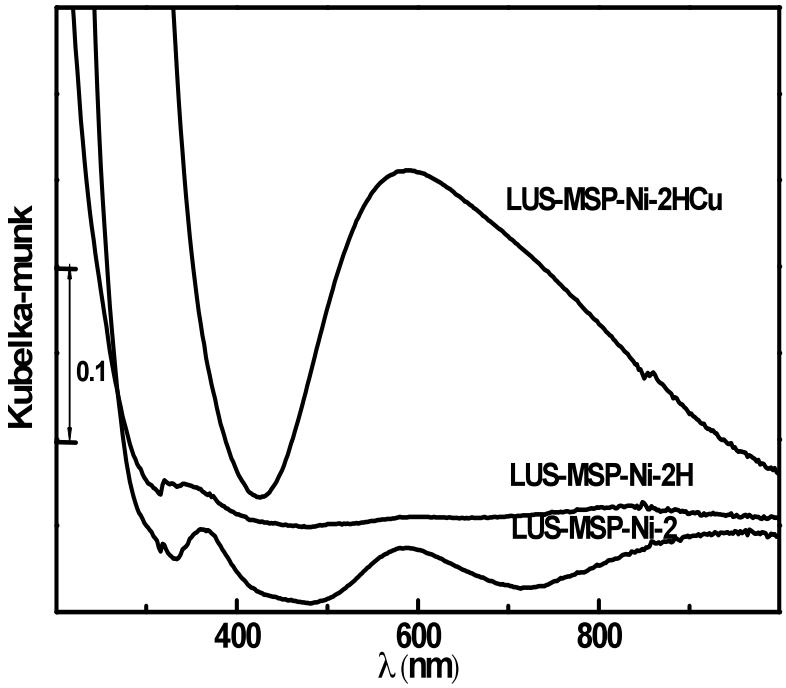

Figure S7. UV-visible absorption spectra of Ni complexes in solution with of different Pren to Ni molar ratios **X** = 1, 2 and 3.

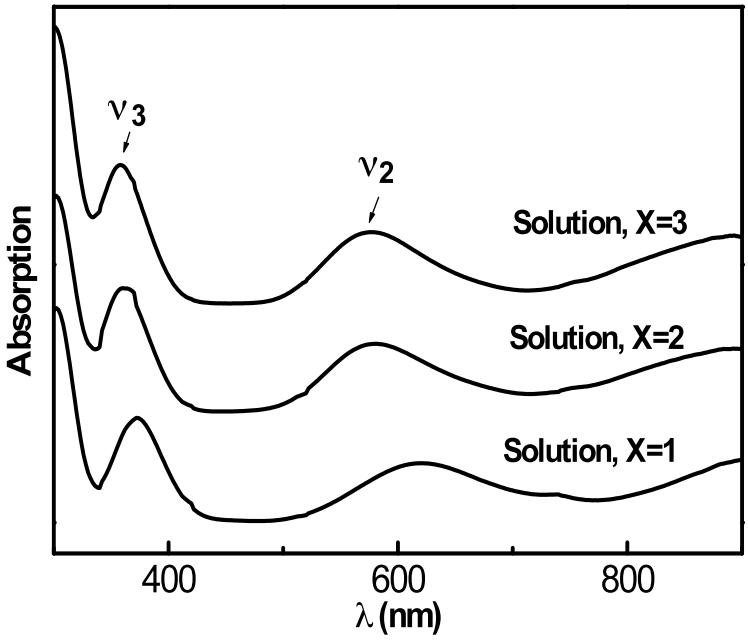

Table S8. UV-visible diffuse reflectance spectra of **OP-Ni-1**, **OP-Ni-2** and **OP-Ni-3**.

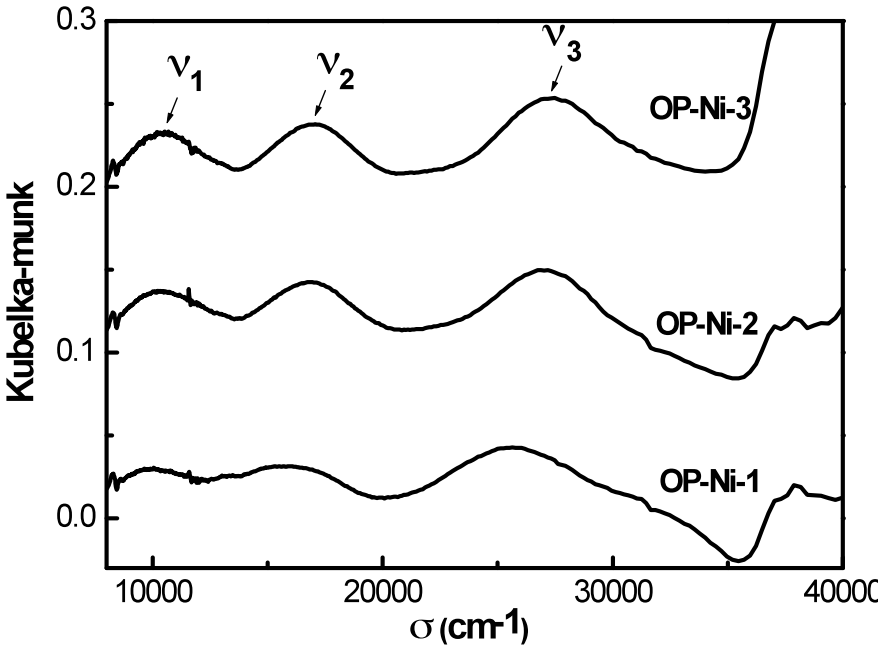

Figure S9. FT-IR spectrum of the precipitate NH_4Cl.

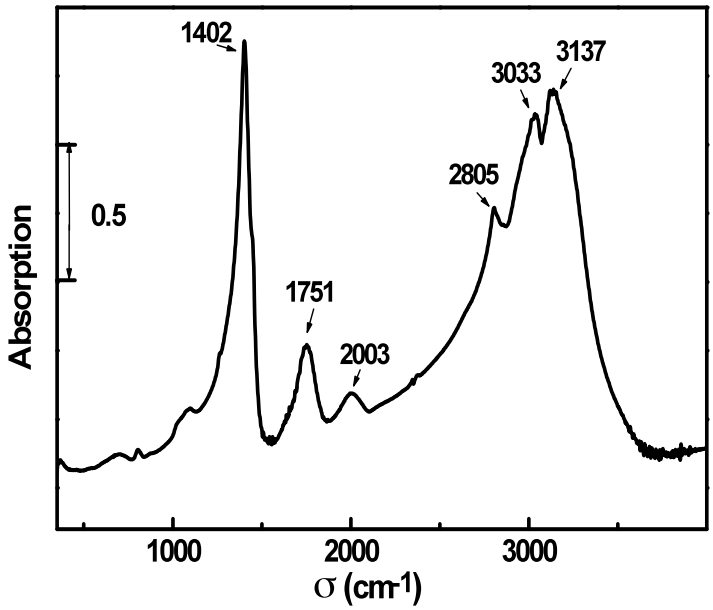

Scheme S1. Simplified correlation diagram between the energy levels of the Ni^{2+} free ion (d^8) and those of the same ion subjected to a crystal field of and octahedral symmetry. Solid line arrows indicate spin-allowed electronic transitions and dotted line arrows spin-forbidden ones.

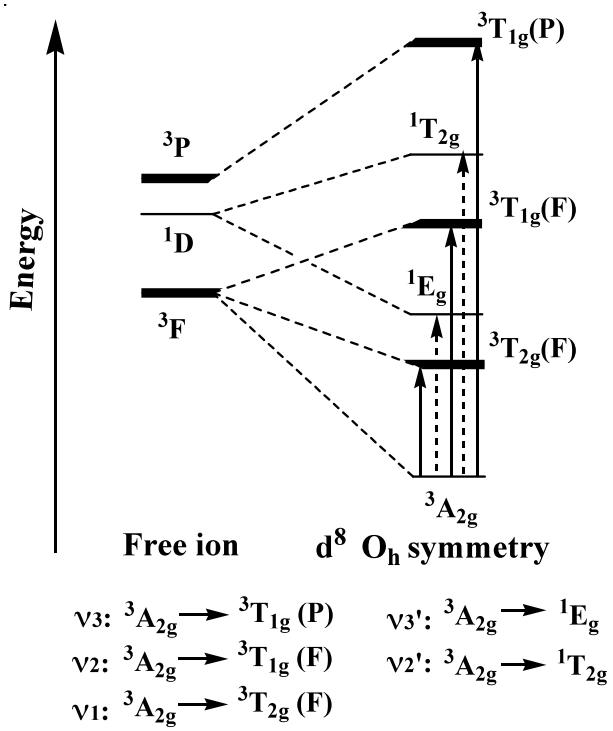

Scheme S2 Reactions of HMDSA with silanol groups of materials (A), and CTMS with silanol groups of materials (B).